

A model comparison of 2D Cartesian and 2D axisymmetric models for positive streamer discharges in air

Zhen Wang^{1,2}, Anbang Sun¹, Jannis Teunissen²

¹State Key Laboratory of Electrical Insulation and Power Equipment, School of Electrical Engineering, Xi'an Jiaotong University, Xi'an, 710049, China,

²Centrum Wiskunde & Informatica, Amsterdam, The Netherlands

E-mail: jannis.teunissen@cwi.nl, anbang.sun@xjtu.edu.cn

Abstract. Simulating streamer discharges in 3D can computationally be very expensive, which is why 2D Cartesian simulations are sometimes used instead, especially when dealing with complex geometries. Although 2D Cartesian simulations can only be used to obtain qualitative results, it is nevertheless interesting to understand how they differ from their 3D or axisymmetric counterparts. We therefore compare 2D Cartesian and axisymmetric simulations of positive streamers in air, using a drift-diffusion-reaction fluid model with the local field approximation. With the same electrode length and width, inception voltages are found to be about a factor two higher in the 2D Cartesian case. When compared at the same applied voltage, the 2D Cartesian streamers are up to four times thinner and slower, their maximal electric field is about 30% lower and their degree of ionization is about 65% lower, with the largest differences occurring at the start of the discharge. When we compare at a similar ratio of applied voltage over inception voltage, velocities become rather similar, and so do the streamer radii at later propagation times. However, the maximal electric field in the 2D Cartesian case is then about 20-30% lower, and the degree of ionization is about 40-50% lower. Finally, we show that streamer branching cannot qualitatively be modeled in a 2D Cartesian geometry.

1. Introduction

Streamer discharges play an important role in the early stages of electric discharges [1], as they generate the first ionized paths that can later become leaders or sparks. Due to their electric field enhancement, streamers can propagate into regions where the electric field is below the breakdown threshold of the insulating medium. Streamer discharges often form a complex tree-like structure with many branched channels. They are widely used in plasma and high voltage technology [2–4], and they appear in thunderstorms as streamer coronas ahead of lightning leaders or as sprite discharges high above thunderclouds [5–7].

Over the past decades, numerical simulations have been widely used to study streamer discharges. Two types of models are commonly used, namely particle models [8–12] and fluid models [13–19]. Simulations have been performed in different computational geometries. 3D Cartesian simulations are the most realistic, but also the most expensive. A fine grid is required to accurately describe the thin charge layers and steep density gradients around streamer channels, and small time steps are required to describe the non-linear evolution of these channels. Axisymmetric simulations are much cheaper to perform, as the solution only has to be evolved in two spatial coordinates (r, z) . For single channels propagating in a straight line, identical results can be obtained as with a full 3D model, see e.g. [20]. On the other hand, real streamer discharges are generally not axisymmetric, for example due to branching or other stochastic effects, or because of their interaction with dielectrics or electrodes. In 2D Cartesian simulations, discharges evolve in x, y coordinates while it is assumed there is no variation in the z -direction. Such simulations therefore describe planar discharges with an infinite extent in the z -direction, which can be a reasonable approximation for surface discharges that are approximately planar.

Because of the high cost of 3D simulations, 2D Cartesian simulations are often used to qualitatively study streamer discharges in complex geometries, which would in reality not be planar. The goal of this paper is to be able to better interpret results of such 2D Cartesian simulations, by comparing them to axisymmetric simulations of positive streamers in air. A planar discharge is expected to have weaker electric field enhancement, because its space charge layer is curved in only one instead of two dimensions. We

aim to understand how this difference affects streamer properties and the conditions for streamer inception.

Below, we briefly mention some of the past work on streamer discharges using 2D Cartesian simulations. Such simulations have frequently been used to describe surface dielectric barrier discharges (SDBDs). We remark that depending on the conditions, SDBDs can be approximately planar but they can also be highly filamentary, see e.g. [21–23].

Soloviev et al used a 2D Cartesian fluid model to study SDBDs in atmospheric air [24, 25]. Singh et al used a 2D Cartesian fluid model to simulate the propagation of streamer discharges towards and then along a solid surface, taking into account charge transport in the dielectric. Meyer et al [26] used a 2D planar fluid model to simulate positive surface streamers and the surface charge distribution on a grounded dielectric barrier. The same model was used to study streamer propagation along a dielectric surface with a wave-like profile in [27]. In [28, 29], positive and negative streamers propagating over a dielectric surface were studied using a 2D Cartesian fluid model. In [30], a two dimensional fluid model (nonPDPSIM) was used to simulate the propagation of discharges through interconnected pores in dielectric materials. In [31], the interaction of positive streamers in air with bubbles floating on liquid surfaces was computationally studied with a 2D Cartesian fluid model.

The outline of the paper is as follows. In section 2, the fluid models and the input data are described. In section 3.1, we compare 2D Cartesian and axisymmetric simulations of positive streamers in air at the same applied voltage. Inception voltages are compared in section 3.2, and simulations are compared at different applied voltages in section 3.3. Finally, we discuss the effect of a 2D Cartesian geometry on streamer branching in section 3.5.

2. Model description

Simulations are performed using Afivo-streamer, a code for drift-diffusion-reaction fluid simulations [14]. The electron density evolves in time as

$$\partial_t n_e = \nabla \cdot (n_e \mu_e \mathbf{E} + D_e \nabla n_e) + S_i - S_a + S_{ph}. \quad (1)$$

Here μ_e and D_e are the electron mobility and diffusion coefficient, which are assumed to be functions of the local electric field. S_{ph} is a non-local photoionization

source term discussed below, and S_i - S_a are source terms due to ionization (S_i) and attachment (S_a) reactions, see section 2.2. Ions and neutral species are assumed to be immobile, and their densities n_j (for $j = 1, 2, \dots$) evolve as

$$\partial_t n_j = S_j, \quad (2)$$

where the source terms S_j are determined by the reaction list, see section 2.2. The electric field is computed as $\mathbf{E} = -\nabla\phi$, where the electric potential ϕ is obtained by solving Poisson's equation using a parallel multigrid solver [14, 32]. The fluid equations are solved with a finite-volume method and explicit time integration, as described in [14].

Photoionization is included according to Zhelenzyak's model [33] using the Helmholtz approximation, using the three-term expansion given in [34]. The parameters used for photoionization are the same as those in [35]. In section 3.5, we additionally show some results with stochastic photoionization, which is implemented as a Monte-Carlo method with discrete photons, see [35] for details.

The Afivo-streamer code includes adaptive mesh refinement (AMR), as described in [14, 36]. As a refinement criterion we use $\alpha(E)\Delta x < 1$, where Δx is the grid spacing and $\alpha(E)$ is the field-dependent ionization coefficient. The mesh is de-refined if $\alpha(E)\Delta x > 0.125$, but only if Δx is smaller than 10 μm .

2.1. Simulation conditions and computational domain

Simulations are performed in artificial air (80% N_2 , 20% O_2) at 1 bar and 300 K. The computational domain used for the 2D Cartesian simulations measures 20 mm \times 10 mm, and a corresponding domain with a radius of 10 mm and a height of 10 mm is employed for the axisymmetric model, see figure 1. We include a rod electrode with a semi-spherical cap to get electric field enhancement. The electrode is 2 mm long and has a radius of 0.2 mm. Note that in the 2D Cartesian model, this rod actually becomes a blade-like electrode.

A Dirichlet boundary condition is used for the electric potential at upper and lower domain boundaries, and a homogeneous Neumann boundary condition is applied on the other boundaries. Homogeneous Neumann boundary conditions are also used for species densities at all domain boundaries.

Figure 1(c) shows that the electric field enhancement at the electrode tip is about 2.6 times higher in the 2D axisymmetric model, namely 310 kV/cm compared to 120 kV/cm. This higher field decays more rapidly, so that farther away from the electrode the field is slightly higher in the 2D Cartesian model (the area under both curves is equal). In both models,

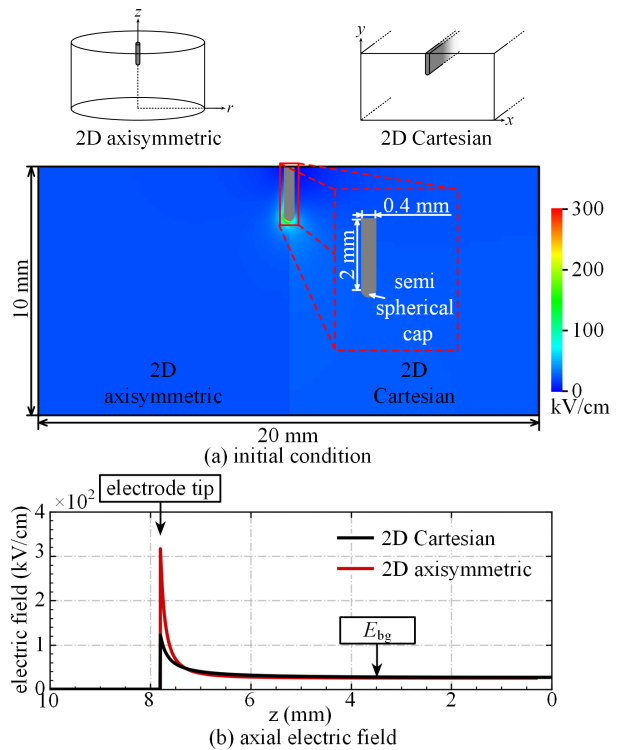


Figure 1: a) Illustration of the 2D Cartesian and 2D axisymmetric computational domains. b) The electrode and the electric field strength in the computational domains. c) Profile of the electric field strength along a central axis in the two models, for an applied voltage of 25 kV/cm. E_{bg} is the average electric field between the plate electrodes.

the electric field far away from the electrode is approximately equal to the average electric field $E_{bg} = 25 \text{ kV/cm}$ between the plate electrodes.

As an initial condition, a homogeneous background ionization density of $1 \times 10^{10} \text{ m}^{-3}$ electrons and positive ions is included, which provides initial free electrons so that a discharge can start.

2.2. Input data

We use Phelps' cross sections for N_2 and O_2 [39, 40, 42, 43] and a relatively simple plasma chemistry, see table 1. Electron transport coefficients (μ_e and D_e) and reaction rates are computed using BOLSIG+ [37, 38]. To get the optical radii of simulated streamers, we included the $\text{N}_2(\text{C}^3\Pi_u \rightarrow \text{B}^3\Pi_g)$ transition in the reaction list, since it is the main source of emitted light [44] in N_2 - O_2 mixtures close to atmospheric pressure.

Table 1: Reactions included in the model. Rate coefficients for k_1 to k_5 were computed using BOLSIG+ [37, 38] from Phelps' cross sections [39, 40], and k_6 to k_8 were obtained from [41].

Reaction	Rate coefficient
$e + N_2 \xrightarrow{k_1} e + e + N_2^+$	$k_1(E/N)$
$e + O_2 \xrightarrow{k_2} e + e + O_2^+$	$k_2(E/N)$
$e + O_2 + O_2 \xrightarrow{k_3} O_2^- + O_2$	$k_3(E/N)$
$e + O_2 \xrightarrow{k_4} O^- + O$	$k_4(E/N)$
$e + N_2 \xrightarrow{k_5} e + N_2(C^3\Pi_u)$	$k_5(E/N)$
$N_2(C^3\Pi_u) + N_2 \xrightarrow{k_6} N_2 + N_2$	$k_6 = 0.13 \times 10^{-16} \text{ m}^3 \text{ s}^{-1}$
$N_2(C^3\Pi_u) + O_2 \xrightarrow{k_7} N_2 + O_2$	$k_7 = 3.0 \times 10^{-16} \text{ m}^3 \text{ s}^{-1}$
$N_2(C^3\Pi_u) \xrightarrow{k_8} N_2(B^3\Pi_g)$	$k_8 = 1/(42 \text{ ns})$

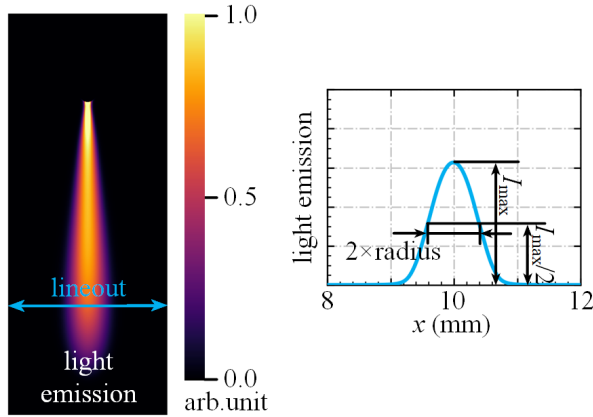


Figure 2: Illustration of how the streamer radius is determined from the light emission profile. At a given position, the full width at half maximum (FWHM) is determined by taking a lineout of the light emission, after which the radius is given by half of the FWHM.

2.3. Computation of streamer radius

There are different definitions of the streamer radius. In this paper we use the optical radius, defined as half of the FWHM (full width at half maximum) of the time-integrated light emission, see figure 2. For axisymmetric simulations, a forward Abel transform is first performed to compute the light emission profile as it would be observed experimentally.

3. Results

3.1. Comparison under the same applied voltage

In this section, 2D Cartesian and 2D axisymmetric simulations of positive streamer discharges are compared using the same applied voltage of $U_0 = 25 \text{ kV}$, which results in a background field of 25 kV/cm . Figure 3

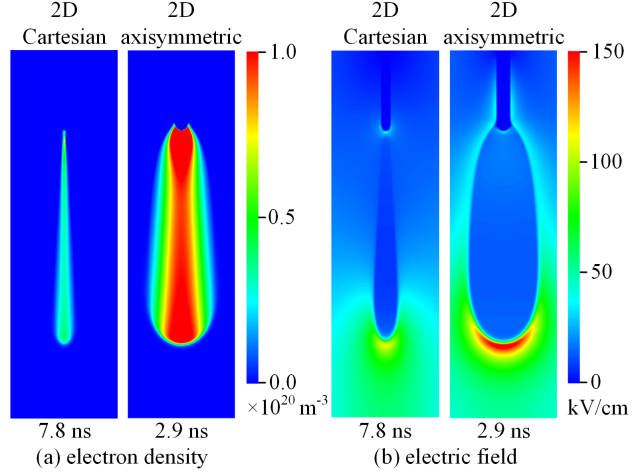


Figure 3: Comparison of electron density and electric field profiles for positive streamer discharges with an applied voltage of $U_0 = 25 \text{ kV/cm}$. Results are shown when the streamers approximately the same position in the the 2D Cartesian and axisymmetric simulations.

shows the electron density and the electric field from a 2D Cartesian simulation at $t = 8.2 \text{ ns}$ and a 2D axisymmetric simulation at $t = 3.2 \text{ ns}$. Corresponding profiles of the maximal electric field, the streamer velocity and the streamer radius are shown in figure 4.

A much smaller streamer radius can be observed in the 2D Cartesian model, as well as a lower electric field at the streamer head and a lower channel conductivity. Normally, one would expect a higher maximal field for a smaller streamer radius, so these differences are caused by the lower electric field enhancement in a 2D Cartesian geometry. Both the radius and the velocity are initially already significantly higher in the axisymmetric model. The maximal electric field relaxes to about 150 kV/cm in the axisymmetric model and to about 100 kV/cm in the 2D Cartesian model.

The two models clearly give rather different results when compared at the same applied voltage. Due to the lower electric field enhancement in a 2D Cartesian geometry we have to use a relatively high voltage to get a discharge started. In the axisymmetric simulations, this voltage is well above the inception voltage, leading to the formation of a wide and fast-propagating discharge channel.

3.2. Comparison of inception voltage

In table 2, inception voltages are compared between the two models, defined as the lowest applied voltage that can initiate a streamer discharge. The same computational domain as before is used, but we vary the electrode length and radius. On average, inception voltages in the 2D Cartesian model are about two times

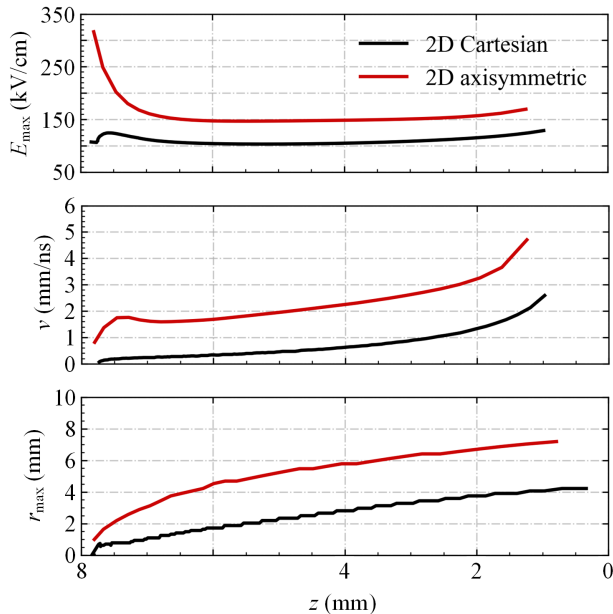


Figure 4: Comparison between 2D Cartesian and axisymmetric simulations for positive streamer discharges at an applied voltage of 25 kV. The streamer head position is determined by the y/r -coordinate of the maximal electric field. Here a second order Savitzky–Golay filter of width five is used to compute a smoothed velocity from the streamer head position versus time data.

Table 2: Streamer inception voltages U_{inc} for different electrode radii and electrode lengths.

	electrode length	electrode radius		
		0.2 mm	0.15 mm	0.1 mm
2D	2 mm	19.0 kV	18.4 kV	17.6 kV
	3 mm	15.8 kV	15.2 kV	14.4 kV
axis.	2 mm	10.4 kV	9.6 kV	8.3 kV
	3 mm	7.9 kV	7.2 kV	6.1 kV

higher than in the axisymmetric model. Note that the inception voltage is somewhat more sensitive to the electrode geometry in the axisymmetric model due to the stronger field enhancement in this geometry.

3.3. Comparison at different voltages

We now compare 2D Cartesian and axisymmetric simulations at different applied voltages, considering two cases: a comparison at the same applied voltage U_0 , and a comparison at a similar value of U_0/U_{inc} , where U_{inc} is the inception voltage. With the electrode geometry used in section 3.1, $U_{\text{inc}} = 19.0$ kV for the 2D Cartesian model and $U_{\text{inc}} = 10.4$ kV for the axisymmetric model, see table 2.

Figure 5 shows the electron density, electric field

and light emission for different applied voltages at the moment the streamer heads reach $z = 2$ mm. In panels (a) and (b), the applied voltages are $U_0 = 21, 22, 23, 24$ and 25 kV. With these voltages, U_0/U_{inc} ranges from 1.11 to 1.32 for the 2D Cartesian model and from 2.0 to 2.4 for the axisymmetric model. In panel (c) axisymmetric results are shown at lower voltages of 12, 13, 14, 15, 16 kV, which correspond to U_0/U_{inc} ranging from 1.15 to 1.54. Figure 6 shows the axial electron density profiles for all these cases, streamer radius, velocity and maximal electric field versus position.

When the 2D Cartesian simulations at 21 kV–25 kV are compared with the axisymmetric simulations at the same voltage, the same large differences as in section 3.1 are observed. The axisymmetric streamer is two to four times wider, with the largest differences occurring near the electrode, and it is also two to four times faster. Furthermore, the maximal electric field E_{max} is about 50% higher in the axisymmetric case and the electron density in the channel is about two to three times higher, see figure 6.

When the 2D Cartesian simulations are compared with the axisymmetric simulations at lower voltages, the streamers have similar velocities. Their radii in the later stages of propagation are similar as well, although initially the 2D Cartesian streamers are much thinner. However, several other differences persist. For the axisymmetric streamers E_{max} is about 20–30% higher and the electron density in the channel is about 50–100% higher, see figure 6. Another important difference is in the decay of the electric field ahead of the streamer, which takes place over a longer distance in a 2D Cartesian geometry. This effect can clearly be seen when comparing figures 5(a) and (c): the region with an electric field strength close to E_{max} is much smaller in the axisymmetric case. This can explain why the 2D Cartesian streamers tend to accelerate more rapidly when they approach the bottom electrode, as there is a larger region ahead of the discharge where the electric field exceeds the critical field.

3.4. Relation between streamer properties

For streamers in air, several (mostly empirical) relations between streamer properties such as velocity, radius and maximal electric field have been established, see e.g. [1, 45]. We now look at a couple of these relations to see whether they change in some particular way for planar (2D Cartesian) discharges.

Figure 7 shows the streamer radius versus velocity. When the applied voltage is near the inception value for both models (21–25 kV for the 2D Cartesian case and 12–16 kV for the axisymmetric case), the velocities increase approximately linearly with the streamer radii. When compared at the same streamer radius, the 2D Cartesian streamers typically have a higher velocity

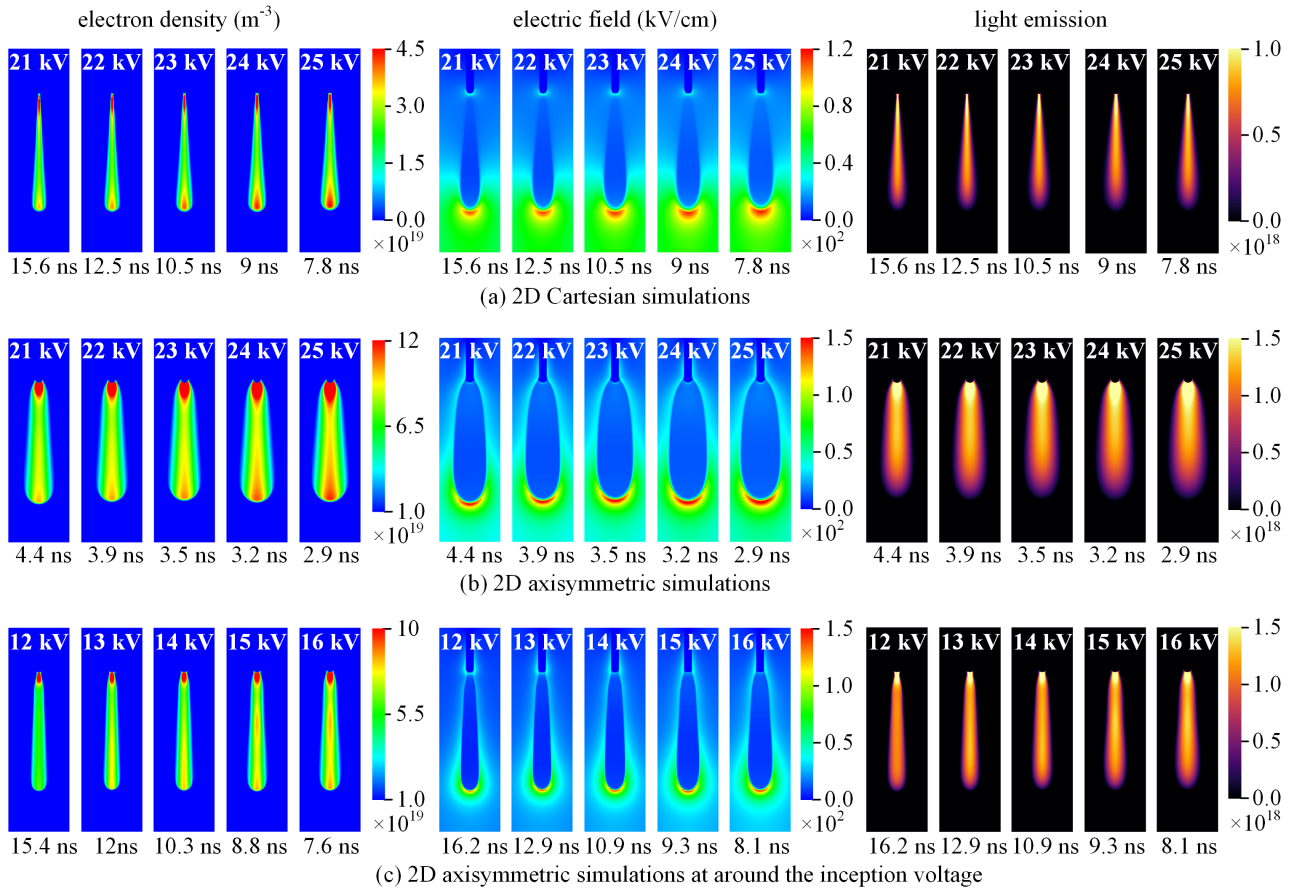


Figure 5: Comparison between 2D Cartesian and axisymmetric models under two groups of applied voltages, which are the group using the same applied voltages and the group using the voltages near the inception value. The electron density, background electric field, and light emission are presented from left to right. The presenting time is selected when the streamer tip reaches $z = 2$ mm. The applied voltages are shown at the top of each plot and the time is at the bottom. Note that different color bars are used.

than the axisymmetric ones, but this is not surprising due to the difference in applied voltage.

Table 3 lists the electron density n_e in the streamer channel (just behind the streamer head) and the maximal electric field strength E_{\max} at the moment the streamers reach $z = 4$ mm. These values are compared with the ionization integral [46–48]

$$n_\alpha(E_{\max}) = \frac{\varepsilon_0}{e} \int_0^{E_{\max}} \alpha_{\text{eff}}(E) dE, \quad (3)$$

and the ratio n_e/n_α is given. This integral is accurate for one-dimensional ionization waves, in which the charge layers are not curved. In axisymmetric or 3D simulations of positive streamers it has been observed that the ratio n_e/n_α is typically about two [49], which was recently related to the role of the displacement current [50]. We find the same ratio $n_e/n_\alpha \approx 2$ for the 2D Cartesian case, even though this geometry lies ‘in between’ a planar 1D ionization wave and a 3D streamer. It is also interesting to note that E_{\max} is not

sensitive to the applied voltage for voltages between 21 kV and 25 kV.

3.5. Branching

Branching determines the morphology of a streamer discharge tree and it influences streamer properties, for example because wider channels are more likely to branch than thinner ones. In previous work [19], we have studied positive streamer branching in artificial air, using a 3D drift-diffusion-reaction fluid model coupled with stochastic photoionization, and we found good agreement with experimental observations. In earlier work, streamer branching has also been computationally studied in a 2D coaxial geometry [51]. An interesting question is therefore to what extent branching can qualitatively be described in a 2D Cartesian geometry.

We expect branching to be significantly weaker in a 2D Cartesian geometry. A first difference is

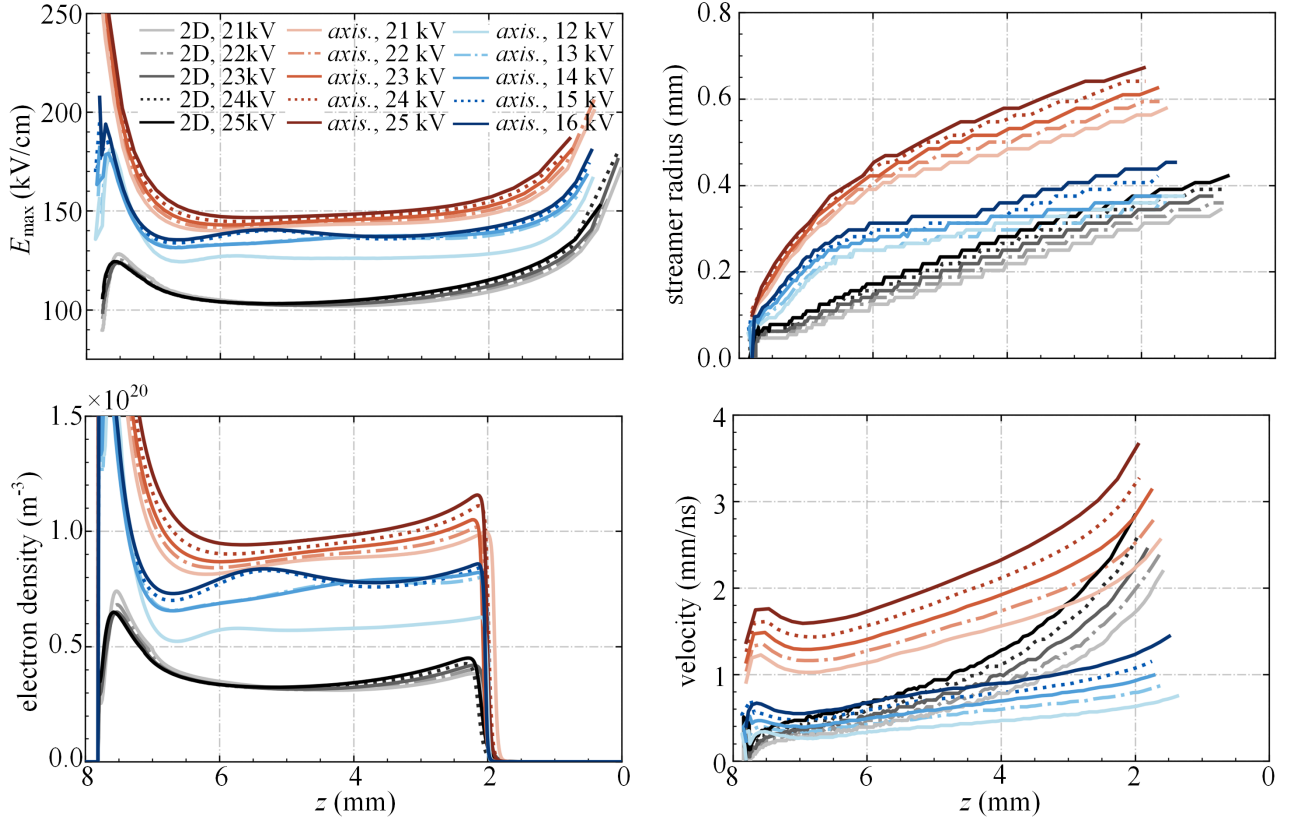


Figure 6: Streamer maximal electric field, radius and velocity versus the streamer head position, for all the cases shown in figure 5. The streamer head position is defined as the vertical coordinate of E_{\max} .

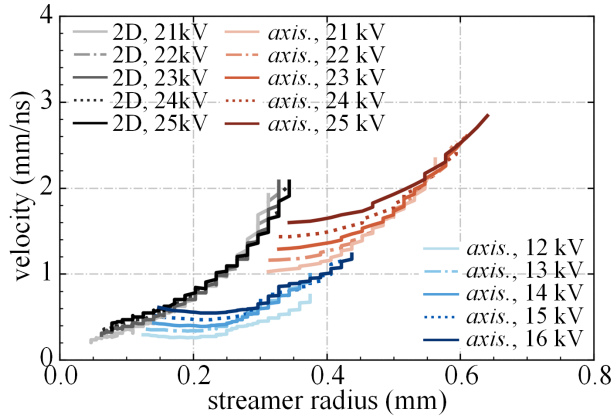


Figure 7: Streamer velocities v versus the maximal streamer radius r_{\max} . The streamer radius is defined based on the light emission, using FWHM method. The same color scheme is used here as in figure 6. The data are extracted when streamer head position is between 7-2 mm.

that charge layers are only curved in one dimension. This curvature drives the branching process through a Laplacian instability, since a protrusion can locally increase the electric field enhancement, see e.g. [1, 52]. In a 2D Cartesian geometry this instability will be significantly weaker. A second difference is that the electric field ahead of a 2D Cartesian streamer has a lower maximum but decays over a longer distance. This leads to less steep electron density gradients, and therefore a reduced probability of branching. A third difference is that higher applied voltages are required to initiate discharges in 2D Cartesian simulations. Streamer can usually grow wider, and thus branch later, with a higher applied voltage.

To test these ideas, we have performed 2D Cartesian simulations with a Monte Carlo photoionization model. By limiting the maximum number of photons n_{photon} that are used to compute the photoionization source term (which is updated every time step), we can artificially increase the amount of noise and induce branching in this model. Figure 8 shows examples of 3D Cartesian simulations from our previous work and examples of branching streamers in 2D Cartesian simulations for different values of n_{photon} . The branching streamers in the 2D Cartesian simulations have a

Voltage (kV)	E_{\max} (kV/cm)	n_e (10^{19} m^{-3})	n_α (10^{19} m^{-3})	n_e/n_α -
2D Cartesian				
21	102.1	3.16	1.46	2.16
22	102.6	3.18	1.49	2.14
23	103.3	3.22	1.53	2.11
24	104.3	3.29	1.58	2.08
25	105.3	3.38	1.64	2.06
Axisymmetric				
21	143.3	8.95	4.70	1.90
22	144.5	9.12	4.83	1.89
23	145.7	9.34	4.96	1.88
24	147.1	9.57	5.11	1.87
25	148.7	9.85	5.29	1.86
Axisymmetric				
12	126.1	5.99	3.09	1.94
13	136.8	7.97	4.05	1.97
14	137.1	7.89	4.08	1.93
15	136.2	7.93	3.99	1.99
16	137.3	8.06	4.09	1.97

Table 3: Degree of ionization n_e , maximal electric field E_{\max} and value of ionization integral n_α , see equation (3). The values were obtained for the cases shown in figures 5– 6 when the streamers reached a vertical position $z = 4 \text{ mm}$.

feather-like shape with many very thin branches, which is completely different from the morphology observed in the 3D simulations and in real discharges in air. This type of branching can only be induced for relatively small values of n_{photon} , showing that branching is suppressed rather strongly. We therefore conclude that 2D Cartesian models cannot qualitatively reproduce streamer branching.

4. Conclusions

In this paper, we have compared 2D Cartesian and 2D axisymmetric simulations of positive streamers. The simulations were performed in air at 1 bar and 300 K, using a drift-diffusion-reaction fluid model. An electrode of the same length and width was used in both geometries, corresponding to a needle in the axisymmetric case and a blade in the 2D Cartesian case. The applied voltage was varied to obtain background fields ranging from 12 kV/cm to 25 kV/cm.

When compared at the same applied voltage, the 2D Cartesian streamers were up to four times thinner and slower, with the largest differences occurring near the start of the discharge. Furthermore, their maximal electric field was about 30% lower and their degree of ionization was about 65% lower. These differences in streamer properties can to some extent be explained

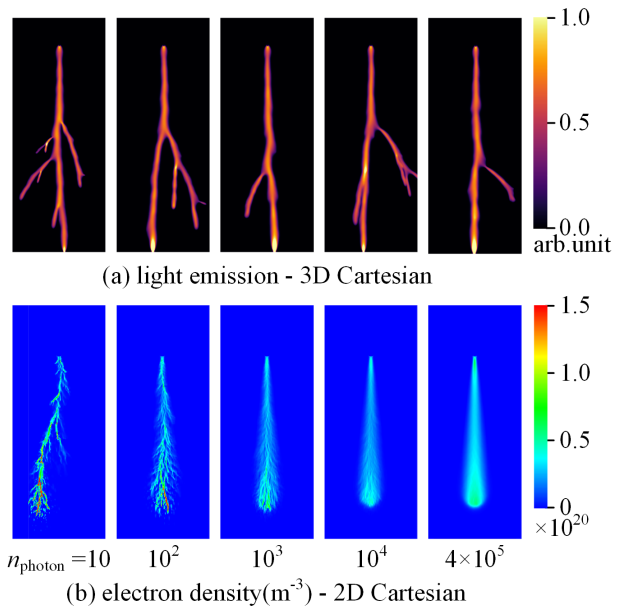


Figure 8: Examples of positive branching streamer in 2D Cartesian model and 3D Cartesian model. The stochastic photoionization is applied in both model to get streamer branching. 5 runs are showed for 3D Cartesian model under the same initial condition, see details in [19]. Different desired weight of superphotons n_{photon} are discussed in 2D Cartesian model, and one run is showed for each value of n_{photon} .

by differences in the respective inception voltages. For several electrode lengths and widths, we found inception voltages to be about twice as high in a 2D Cartesian geometry, due to the weaker electric field enhancement.

We therefore also performed a comparison at a similar ratio of applied voltage over inception voltage. Velocities then became rather similar in the two types of models, and so did the streamer radii at later propagation times. However, the maximal electric field in the 2D Cartesian case was still about 20-30% lower, and the degree of ionization was about 40-50% lower.

We have briefly looked at several relations between streamer properties, such as velocity, radius, maximal electric field and degree of ionization. Furthermore, we have show that streamer branching cannot qualitatively be reproduced in a 2D Cartesian simulations. Branching only occurs when strong noise is added to such simulations, and the resulting branches are much thinner than in real discharges in air.

Our findings can help to interpret the results of 2D Cartesian simulations, which can be a valuable tool to qualitatively study streamer phenomena under conditions that are computationally too expensive to

simulate in full 3D.

References

- [1] Sander Nijdam, Jannis Teunissen, and Ute Ebert. The physics of streamer discharge phenomena. *Plasma Sources Science and Technology*, 29(10):103001, 2020.
- [2] A Fridman, A Chirokov, and A Gutsol. Non-thermal atmospheric pressure discharges. *Journal of Physics D: Applied Physics*, 38(2):R1, 2005.
- [3] Peter J Bruggeman, Felipe Iza, and Ronny Brandenburg. Foundations of atmospheric pressure non-equilibrium plasmas. *Plasma Sources Science and Technology*, 26(12):123002, 2017.
- [4] Douyan Wang and Takao Namihira. Nanosecond pulsed streamer discharges: II. Physics, discharge characterization and plasma processing. *Plasma Sources Science and Technology*, 29(2):023001, February 2020.
- [5] Steven A. Cummer, Nicolas Jaugey, Jingbo Li, Walter A. Lyons, Thomas E. Nelson, and Elizabeth A. Gerken. Submillisecond imaging of sprite development and structure. *Geophysical Research Letters*, 33(4), 2006.
- [6] Matthew G McHarg, Hans C Stenbaek-Nielsen, and Takeshi Kammae. Observations of streamer formation in sprites. *Geophysical Research Letters*, 34(6), 2007.
- [7] Alejandro Luque and Ute Ebert. Emergence of sprite streamers from screening-ionization waves in the lower ionosphere. *Nature Geoscience*, 2(11):757–760, November 2009.
- [8] D. V. Rose, D. R. Welch, R. E. Clark, C. Thoma, W. R. Zimmerman, N. Bruner, P. K. Rambo, and B. W. Ather-ton. Towards a fully kinetic 3D electromagnetic particle-in-cell model of streamer formation and dynamics in high-pressure electronegative gases. *Physics of Plasmas*, 18(9):093501, September 2011.
- [9] Jannis Teunissen and Ute Ebert. 3d pic-mcc simulations of discharge inception around a sharp anode in nitrogen/oxygen mixtures. *Plasma Sources Science and Technology*, 25(4):044005, 2016.
- [10] Vladimir Kolobov and Robert Arslanbekov. Electrostatic PIC with adaptive Cartesian mesh. *Journal of Physics: Conference Series*, 719:012020, May 2016.
- [11] Dmitry Levko, Michael Pachui, and Laxminarayan L Raja. Particle-in-cell modeling of streamer branching in CO₂ gas. *Journal of Physics D: Applied Physics*, 50(35):354004, September 2017.
- [12] J Stephens, M Abide, A Fierro, and A Neuber. Practical considerations for modeling streamer discharges in air with radiation transport. *Plasma Sources Science and Technology*, 27(7):075007, July 2018.
- [13] Natalia Yu Babaeva, Dmitry V Tereshonok, and George V Naidis. Fluid and hybrid modeling of nanosecond surface discharges: Effect of polarity and secondary electrons emission. *Plasma Sources Science and Technology*, 25(4):044008, July 2016.
- [14] Jannis Teunissen and Ute Ebert. Simulating streamer discharges in 3d with the parallel adaptive afivo framework. *Journal of Physics D: Applied Physics*, 50(47):474001, 2017.
- [15] J-M Plewa, O Eichwald, O Ducasse, P Dessante, C Jacobs, N Renon, and M Yousfi. 3D streamers simulation in a pin to plane configuration using massively parallel computing. *Journal of Physics D: Applied Physics*, 51(9):095206, March 2018.
- [16] Robert Marskar. An adaptive Cartesian embedded boundary approach for fluid simulations of two- and three-dimensional low temperature plasma filaments in complex geometries. *Journal of Computational Physics*, 388:624–654, July 2019.
- [17] A Yu Starikovskiy and N L Aleksandrov. How pulse polarity and photoionization control streamer discharge development in long air gaps. *Plasma Sources Science and Technology*, 29(7):075004, July 2020.
- [18] Ryo Ono and Atsushi Komuro. Generation of the single-filament pulsed positive streamer discharge in atmospheric-pressure air and its comparison with two-dimensional simulation. *Journal of Physics D: Applied Physics*, 53(3):035202, January 2020.
- [19] Zhen Wang, Siebe Dijkstra, Yihao Guo, Martijn van der Leegte, Anbang Sun, Ute Ebert, Sander Nijdam, and Jannis Teunissen. Quantitative modeling of streamer discharge branching in air. *Plasma Sources Science and Technology*, 2023.
- [20] Zhen Wang, Anbang Sun, and Jannis Teunissen. A comparison of particle and fluid models for positive streamer discharges in air. *Plasma Sources Science and Technology*, 31(1):015012, 2022.
- [21] A Sobota, A Lebouvier, N J Kramer, E M Van Veldhuizen, W W Stoffels, F Manders, and M Haverlag. Speed of streamers in argon over a flat surface of a dielectric. *Journal of Physics D: Applied Physics*, 42(1):015211, January 2009.
- [22] S A Stepanyan, A Yu Starikovskiy, N A Popov, and S M Starikovskaia. A nanosecond surface dielectric barrier discharge in air at high pressures and different polarities of applied pulses: Transition to filamentary mode. *Plasma Sources Science and Technology*, 23(4):045003, June 2014.
- [23] Ch Ding, A Jean, N A Popov, and S M Starikovskaia. Fine structure of streamer-to-filament transition in high-pressure nanosecond surface dielectric barrier discharge. *Plasma Sources Science and Technology*, 31(4):045013, April 2022.
- [24] VR Soloviev and VM Krivtsov. Surface barrier discharge modelling for aerodynamic applications. *Journal of Physics D: Applied Physics*, 42(12):125208, 2009.
- [25] VR Soloviev and VM Krivtsov. Mechanism of streamer stopping in a surface dielectric barrier discharge. *Plasma Physics Reports*, 40:65–77, 2014.
- [26] Hans Kristian Meyer, Frank Mauseth, Robert Marskar, Atle Pedersen, and Andreas Blaszczyk. Streamer and surface charge dynamics in non-uniform air gaps with a dielectric barrier. *IEEE Transactions on Dielectrics and Electrical Insulation*, 26(4):1163–1171, 2019.
- [27] Hans Kristian Hygen Meyer, Robert Marskar, Henrik Gjerdal, and Frank Mauseth. Streamer propagation along a profiled dielectric surface. *Plasma Sources Science and Technology*, 29(11):115015, 2020.
- [28] Xiaoran Li, Anbang Sun, Guanjun Zhang, and Jannis Teunissen. A computational study of positive streamers interacting with dielectrics. *Plasma Sources Science and Technology*, 29(6):065004, 2020.
- [29] Xiaoran Li, Anbang Sun, and Jannis Teunissen. A computational study of negative surface discharges: Characteristics of surface streamers and surface charges. *IEEE Transactions on Dielectrics and Electrical Insulation*, 27(4):1178–1186, 2020.
- [30] Juliusz Kruszelnicki, Runchu Ma, and Mark J Kushner. Propagation of atmospheric pressure plasmas through interconnected pores in dielectric materials. *Journal of Applied Physics*, 129(14), 2021.
- [31] Natalia Yu Babaeva, George V Naidis, and Mark J Kushner. Interaction of positive streamers in air with bubbles floating on liquid surfaces: conductive and dielectric bubbles. *Plasma Sources Science and Technology*, 27(1):015016, 2018.
- [32] Jannis Teunissen and Francesca Schiavello. Geometric

- multigrid method for solving poisson's equation on octree grids with irregular boundaries. *Computer Physics Communications*, 286:108665, 2023.
- [33] MB Zhelezniak, A Kh Mnatsakanian, and Sergei Vasil'evich Sizykh. Photoionization of nitrogen and oxygen mixtures by radiation from a gas discharge. *High Temperature Science*, 20(3):357–362, 1982.
- [34] Anne Bourdon, VP Pasko, NY Liu, Sébastien Célestin, Pierre Ségur, and Emmanuel Marode. Efficient models for photoionization produced by non-thermal gas discharges in air based on radiative transfer and the helmholtz equations. *Plasma Sources Science and Technology*, 16(3):656, 2007.
- [35] Behnaz Bagheri and Jannis Teunissen. The effect of the stochasticity of photoionization on 3d streamer simulations. *Plasma Sources Science and Technology*, 28(4):045013, 2019.
- [36] Jannis Teunissen and Ute Ebert. Afivo: A framework for quadtree/octree amr with shared-memory parallelization and geometric multigrid methods. *Computer Physics Communications*, 233:156–166, 2018.
- [37] GJM Hagelaar and LC Pitchford. Solving the boltzmann equation to obtain electron transport coefficients and rate coefficients for fluid models. *Plasma Sources Science and Technology*, 14(4):722, 2005.
- [38] Bolsig+ solver. www.lxcat.net, ver. 11/2019.
- [39] AV Phelps and LC Pitchford. Anisotropic scattering of electrons by n_2 and its effect on electron transport. *Physical Review A*, 31(5):2932, 1985.
- [40] Phelps database (N_2, O_2). www.lxcat.net, retrieved on March 30, 2021.
- [41] S. Pancheshnyi, M. Nudnova, and A. Starikovskii. Development of a cathode-directed streamer discharge in air at different pressures: Experiment and comparison with direct numerical simulation. *Physical Review E*, 71(1), January 2005.
- [42] S. A. Lawton and A. V. Phelps. Excitation of the $b\ 1\Sigma^+g$ state of O_2 by low energy electrons. *The Journal of Chemical Physics*, 69(3):1055–1068, August 1978.
- [43] L. C. Pitchford and A. V. Phelps. Comparative calculations of electron-swarm properties in N_2 at moderate E/N values. *Physical Review A*, 25(1):540–554, January 1982.
- [44] SV Pancheshnyi, SV Sobakin, SM Starikovskaya, and A Yu Starikovskii. Discharge dynamics and the production of active particles in a cathode-directed streamer. *Plasma Physics Reports*, 26(12):1054–1065, 2000.
- [45] G. V. Naidis. Positive and negative streamers in air: Velocity-diameter relation. *Physical Review E*, 79(5), May 2009.
- [46] Ute Ebert, Wim van Saarloos, and Christiane Caroli. Streamer Propagation as a Pattern Formation Problem: Planar Fronts. *Physical Review Letters*, 77(20):4178–4181, November 1996.
- [47] N Yu Babaeva and G V Naidis. Two-dimensional modelling of positive streamer dynamics in non-uniform electric fields in air. *Journal of Physics D: Applied Physics*, 29(9):2423–2431, September 1996.
- [48] G V Naidis. Modelling of plasma chemical processes in pulsed corona discharges. *Journal of Physics D: Applied Physics*, 30(8):1214–1218, April 1997.
- [49] Xiaoran Li, Baohong Guo, Anbang Sun, Ute Ebert, and Jannis Teunissen. A computational study of steady and stagnating positive streamers in N_2-O_2 mixtures. *Plasma Sources Sci. Technol.*, page 15, 2022.
- [50] Dennis Bouwman, Hani Francisco, and Ute Ebert. Estimating the properties of single positive air streamers from measurable parameters. *Plasma Sources Science and Technology*, 32(7):075015, July 2023.
- [51] Zhongmin Xiong and Mark J Kushner. Branching and path-deviation of positive streamers resulting from statistical photon transport. *Plasma Sources Science and Technology*, 23(6):065041, October 2014.
- [52] U Ebert, F Brau, G Derks, W Hundsdorfer, C-Y Kao, C Li, A Luque, B Meulenbroek, S Nijdam, V Ratushnaya, L Schäfer, and S Tanveer. Multiple scales in streamer discharges, with an emphasis on moving boundary approximations. *Nonlinearity*, 24(1):C1–C26, January 2011.